Revisiting Clockwork Model: A Review of Theoretical Foundations and Experimental Progress

Gayatri Ghosh

Department of Physics, Cachar College, Assam University, India

And

Maxim Khlopov

Virtual Institute of Astroparticle Physics, 75018 Paris, France Institute of Physics, Southern Federal University, Rostov on Don 344090, Russia National Research Nuclear University MEPHI, 115409 Moscow, Russia

International Conference on Neutrinos and Dark Matter (NuDM- 2024), Dec 11 – 14, 2024

Cairo - Egypt

- Clockwork fermions constitute a groundbreaking theoretical framework in high-energy physics,
- addressing profound challenges such as the hierarchy problem and the origin of small neutrino masses.
- The clockwork mechanism introduces elegant solutions to mass hierarchies, leveraging novel theoretical
- constructs that yield distinctive phenomenological signatures.
- Recent collider searches and direct detection experiments have imposed stringent constraints on
- clockwork models, guiding the parameter space for further exploration.
- Beyond particle physics, clockwork fermions offer intriguing implications for dark matter and cosmology,
- underscoring their interdisciplinary significance.

Gayatri Ghosh * and Maxim Khlopov Posted Date: 15 August 2024 doi: 10.20944/preprints202408.1122.v1
Keywords: clockwork fermions; mass hierarchies; dark matter; invisible axion; Beyond the Standard model

1. Introduction

- Clockwork models rely on the idea of generating exponentially suppressed interactions through a linear chain of fields, each coupling only to its nearest neighbor.
- The basic idea of the clockwork mechanism [1] involves a series of fields (referred to as gears)
- Consider a supersymmetric theory [2,3] with a series of chiral superfields Φi (i = 0, 1, . . . , N). The superpotential can be written as:

$$W = \sum_{i=0}^{N-1} \left(k\Phi_i\Phi_{i+1} + m_i\Phi_i^2 \right)$$

- In the clockwork mechanism, fields are arranged in a linear chain of sites, with nearest-neighbor interactions mediated by a coupling constant.

$$\mathcal{L} = \sum_{j=0}^{N-1} \left(\overline{\psi}_j i\gamma^\mu \partial_\mu \psi_j - m\overline{\psi}_j \psi_j - \frac{k}{2}\left(\overline{\psi}_j \psi_{j+1} + \overline{\psi}_{j+1} \psi_j \right) \right), \tag{1}$$

where ψ_j represents the fermion field at site j, m is the mass parameter, and k is the coupling between nearest-neighbor sites.

By diagonalizing the mass matrix, we find the mass eigenvalues to be exponentially spaced:

$$m_n \approx m\left(1 - \frac{k}{m}\cos\left(\frac{\pi n}{N}\right)\right), \tag{2}$$

where n indexes the mass eigenstates.

For instance, the suppression factor for the N-th site is given by:

$$\epsilon \sim \left(\frac{k}{m}\right)^N. \tag{3}$$

For scalar fields, the Lagrangian can be written as:

$$\mathcal{L} = \sum_{j=0}^{N-1} \left(\frac{1}{2} \partial_\mu \phi_j \partial^\mu \phi_j - \frac{1}{2} m^2 \phi_j^2 - \frac{k}{2} (\phi_j \phi_{j+1} + \phi_{j+1} \phi_j) \right), \tag{4}$$

where φ_j represents the scalar field at site j.

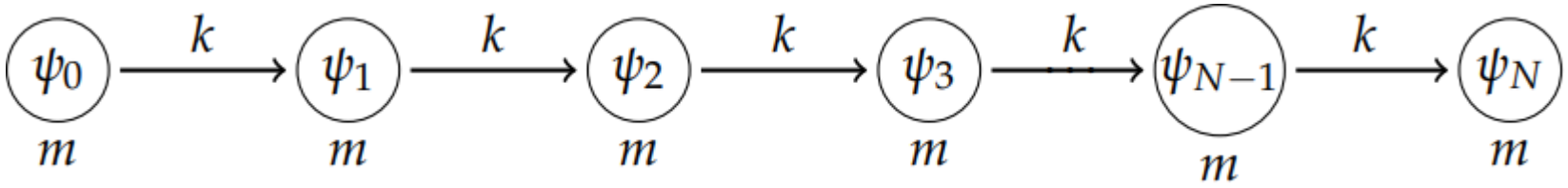

The strong CP problem [7] arises from the QCD Lagrangian, which allows for a term that could lead to CP violation:

$$\mathcal{L}_\theta = \theta \frac{g^2}{32\pi^2} G_{\mu\nu} \tilde{G}^{\mu\nu}$$

These fields interact in a way described by a potential:

$$V = \sum_{i=0}^{N-1} \left(\frac{1}{2} m_i^2 (a_{i+1} - q a_i)^2 \right)$$

The physical axion aphys is a linear combination of these fields and has an effective decay constant given by:

$$f_{\text{phys}} = q^N f$$

where f is the decay constant of the original axion field.

2. Theoretical Background

Consider a simple scalar clockwork model with N + 1 fields φi (i = 0, 1, ..., N). The Lagrangian is given by:

$$\mathcal{L} = \sum_{i=0}^{N} \frac{1}{2}(\partial_\mu \phi_i)^2 - \sum_{i=0}^{N-1} \frac{1}{2} m^2 (\phi_i - q\phi_{i+1})^2, \qquad (5)$$

2.1. Clockwork Fermion Model

The Lagrangian describing the clockwork fermions can be written as

$$\mathcal{L} = \sum_{j=0}^{N} \left(\overline{\psi}_j i\gamma^\mu \partial_\mu \psi_j - m\overline{\psi}_j \psi_j \right) - \sum_{j=0}^{N-1} \left(\frac{k}{2} \overline{\psi}_j \psi_{j+1} + \frac{k}{2} \overline{\psi}_{j+1} \psi_j \right), \tag{6}$$

where m is the mass parameter and k is the coupling constant between nearest-neighbor sites. The mass matrix for the fermion fields is:

$$M = \begin{pmatrix} m & \frac{k}{2} & 0 & \cdots & 0 \\ \frac{k}{2} & m & \frac{k}{2} & \cdots & 0 \\ 0 & \frac{k}{2} & m & \cdots & 0 \\ \vdots & \vdots & \vdots & \ddots & \frac{k}{2} \\ 0 & 0 & 0 & \frac{k}{2} & m \end{pmatrix}. \tag{7}$$

Diagonalizing this mass matrix gives the mass eigenvalues:

$$m_n \approx m\left(1 - \frac{k}{m}\cos\left(\frac{\pi n}{N}\right)\right), \tag{8}$$

If we consider an interaction term involving the field at the N-th site, ψ_N, the effective coupling can be exponentially suppressed as:

$$g_{\text{eff}} \sim g\left(\frac{k}{m}\right)^N, \tag{9}$$

where g is the original coupling constant. Consider a series of scalar fields, φ_j , arranged in a similar chain. The Lagrangian is given by:

$$\mathcal{L} = \sum_{j=0}^{N}\left(\frac{1}{2}\partial_\mu\phi_j\partial^\mu\phi_j - \frac{1}{2}m^2\phi_j^2\right) - \sum_{j=0}^{N-1}\left(\frac{k}{2}\phi_j\phi_{j+1} + \frac{k}{2}\phi_{j+1}\phi_j\right). \tag{10}$$

The Lagrangian for a simple Dirac clockwork fermion model can be written as:

$$\mathcal{L} = \sum_{i=0}^{N}\overline{\psi}_i i\gamma^\mu\partial_\mu\psi_i - \sum_{i=0}^{N-1} m(\overline{\psi}_i\psi_{i+1} + \text{h.c.}), \tag{11}$$

3. Clockwork Mechanism in Particle Physics

3.1. Higgs Hierarchy Problem

In Figure 1 the blue curve represents a gear with a relatively fast suppression rate. The influence of this gear diminishes quickly as x increases. The red gear has a slower suppression rate compared to the blue gear, meaning its influence persists longer. The green gear has the slowest suppression rate among the three, maintaining its influence over the longest range.

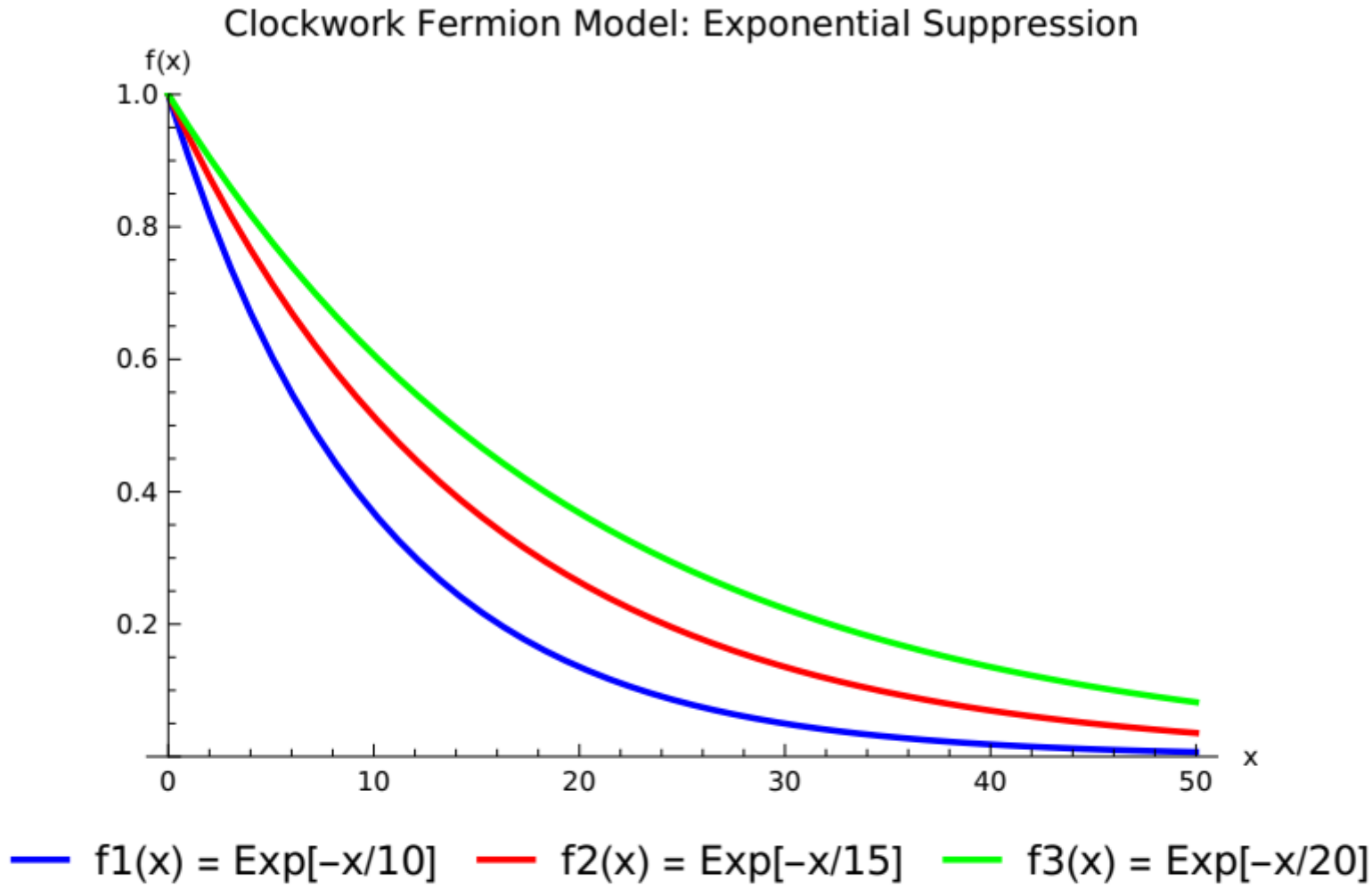

Figure 1. Figure 1 visually represents how the clockwork fermion model can dilute the influence of each gear over increasing distances, addressing the hierarchy problem by naturally reducing large scales.

In a clockwork Higgs model, the Higgs field is part of a clockwork chain, with the effective coupling to the zero-mode being suppressed by a factor of q^{-N}
Consider a clockwork chain for the Higgs field φi with the Lagrangian:

$$\mathcal{L} = \sum_{i=0}^{N} (\partial_\mu \phi_i)^\dagger (\partial^\mu \phi_i) - \sum_{i=0}^{N-1} m^2 |\phi_i - q\phi_{i+1}|^2, \tag{12}$$

where m and q are parameters of the clockwork mechanism. The Higgs mass mH receives quantum corrections from loops of other particles. In a simplified form, the correction can be written as:

$$\delta m_H^2 \sim \frac{\Lambda^2}{16\pi^2} \left(\lambda_t^2 - \lambda_b^2 + \lambda_W^2 - \lambda_Z^2 \right)$$

where: • Λ is the cutoff scale, possibly the Planck scale (~ 10^{19}GeV), • λ_i are the couplings of the Higgs to various particles (top quark, bottom quark, W and Z bosons).

For the Higgs mass to remain around the electroweak scale, δm^2_H must be fine-tuned to cancel out to a large degree, which seems unnatural. Consider a set of N + 1 scalar fields φ_i with the Lagrangian:

$$\mathcal{L} = \sum_{i=0}^{N} \frac{1}{2}(\partial_\mu \phi_i)^2 - \frac{1}{2} m_i^2 \phi_i^2 - \sum_{i=0}^{N-1} \frac{k^2}{2}(\phi_{i+1} - q\phi_i)^2$$

Here:

- m_i are the masses of the scalar fields,
- k is a coupling constant,

Higgs Hierarchy Plot Using Clockwork Fermions

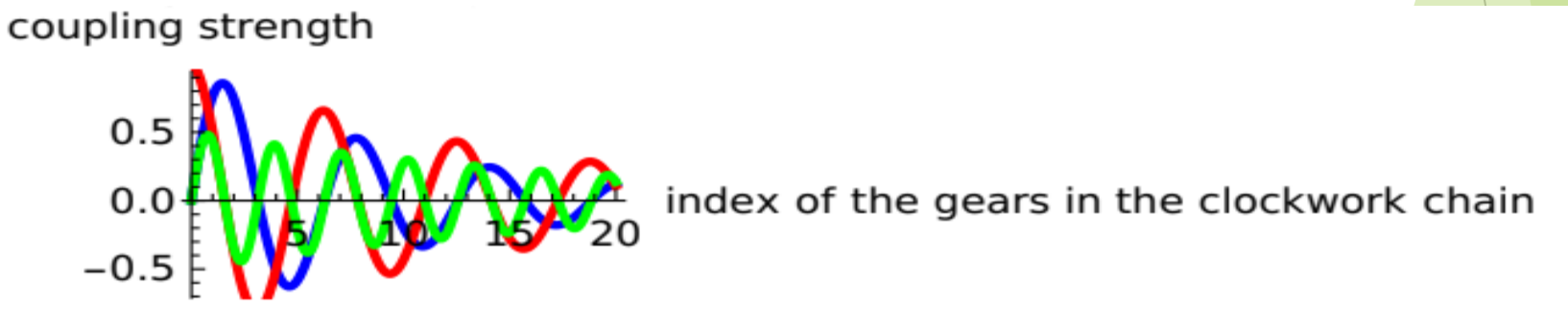

In Figure 2 we illustrate the key idea of the clockwork mechanism: by introducing a series of interacting fields (the gears), it is possible to generate a wide range of behaviors and coupling strengths. This diversity allows the model to effectively address the hierarchy problem by diluting the initial scale down to a much smaller scale in a controlled manner.

3.2. Neutrino Masses and Mixings

Consider a clockwork chain for right-handed neutrinos NRi, with the Lagrangian:

$$\mathcal{L} = \sum_{i=0}^{N} \overline{N}_{Ri} i\gamma^{\mu} \partial_{\mu} N_{Ri} - \sum_{i=0}^{N-1} m(\overline{N}_{Ri} N_{R(i+1)} + \text{h.c.}), \tag{13}$$

where m is the mass parameter.

The Lagrangian for the clockwork mechanism involving neutrinos can be written as

$$\mathcal{L} = \sum_{i=0}^{N} \left[\overline{\nu_{L,i}} i\gamma^{\mu} \partial_{\mu} \nu_{L,i} + \overline{\nu_{R,i}} i\gamma^{\mu} \partial_{\mu} \nu_{R,i} \right] - \sum_{i=0}^{N-1} \left[m\overline{\nu_{L,i+1}} \nu_{R,i} + k\overline{\nu_{L,i}} \nu_{R,i} + \text{h.c.} \right]$$

The mass matrix M for the neutrino fields can be represented as:

$$M = \begin{pmatrix} 0 & k & 0 & 0 & \cdots & 0 \\ m & 0 & k & 0 & \cdots & 0 \\ 0 & m & 0 & k & \cdots & 0 \\ 0 & 0 & m & 0 & \cdots & 0 \\ \vdots & \vdots & \vdots & \vdots & \ddots & k \\ 0 & 0 & 0 & 0 & m & 0 \end{pmatrix}.$$

The PMNS matrix UPMNS is a unitary matrix that relates the flavor eigenstates to the mass eigenstates:

$$\begin{pmatrix} \nu_e \\ \nu_\mu \\ \nu_\tau \end{pmatrix} = U_{\text{PMNS}} \begin{pmatrix} \nu_1 \\ \nu_2 \\ \nu_3 \end{pmatrix}$$

The PMNS matrix is typically parameterized as:

$$U_{\mathrm{PMNS}} = \begin{pmatrix} U_{e1} & U_{e2} & U_{e3} \\ U_{\mu 1} & U_{\mu 2} & U_{\mu 3} \\ U_{\tau 1} & U_{\tau 2} & U_{\tau 3} \end{pmatrix} = \begin{pmatrix} c_{12}c_{13} & s_{12}c_{13} & s_{13}e^{-i\delta} \\ -s_{12}c_{23} - c_{12}s_{23}s_{13}e^{i\delta} & c_{12}c_{23} - s_{12}s_{23}s_{13}e^{i\delta} & s_{23}c_{13} \\ s_{12}s_{23} - c_{12}c_{23}s_{13}e^{i\delta} & -c_{12}s_{23} - s_{12}c_{23}s_{13}e^{i\delta} & c_{23}c_{13} \end{pmatrix}$$

$$U_{\mathrm{PMNS}} = \begin{pmatrix} U_{e1} & U_{e2} & U_{e3} \\ U_{\mu 1} & U_{\mu 2} & U_{\mu 3} \\ U_{\tau 1} & U_{\tau 2} & U_{\tau 3} \end{pmatrix}$$

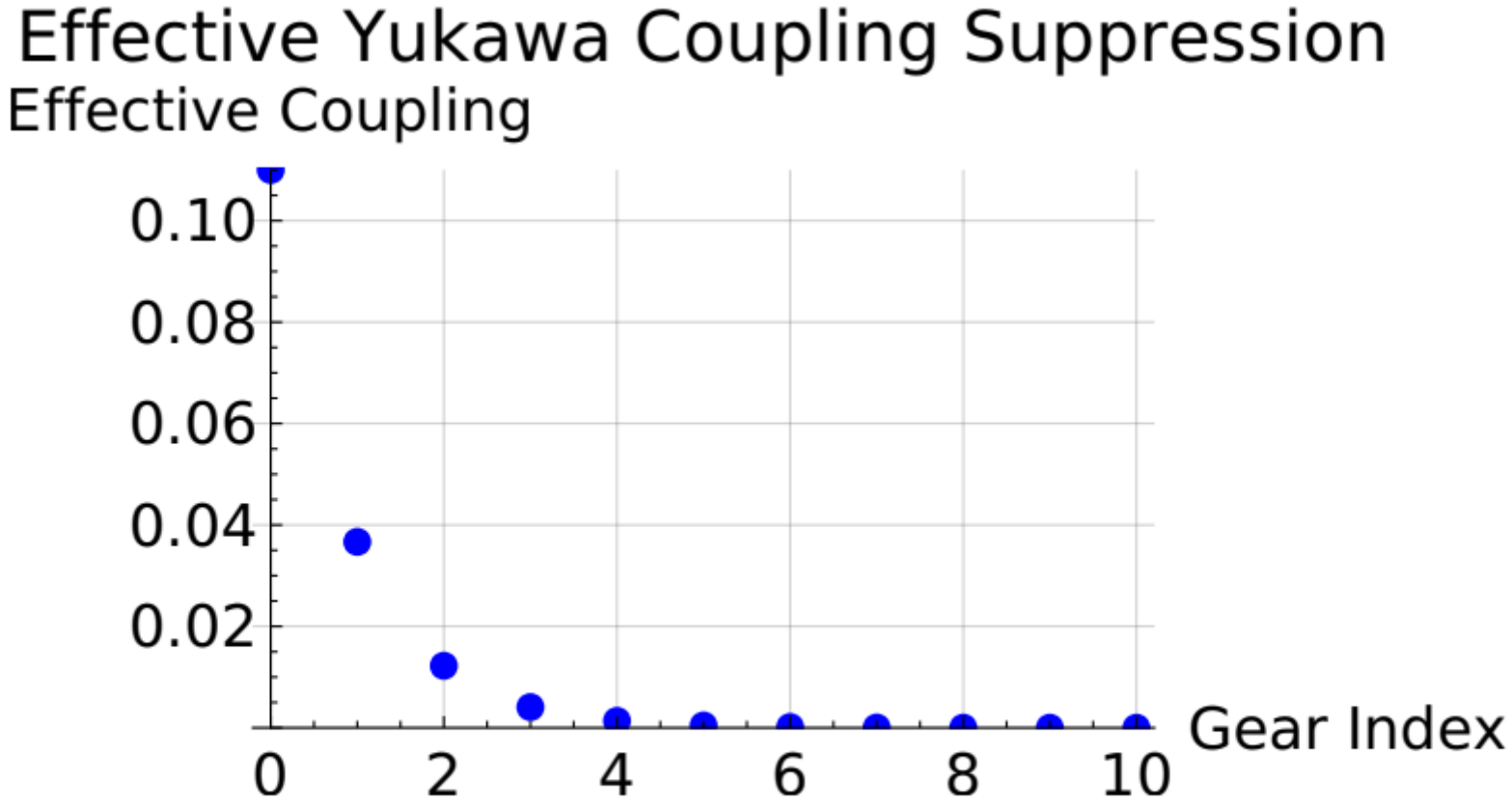

Figure 3. Figure 3 represents a rapid decrease in the effective Yukawa coupling as the gear index increases. This exponential suppression means that even with an initial Yukawa coupling of $y_0 = 0.1$, the effective coupling can become very small after just a few gears.

The clockwork mechanism involves a series of fields (gears) that are coupled in such a way that the effective coupling constant decreases exponentially along the chain. Mathematically, the effective coupling after k gears can be represented as: $y_{eff(k)} = y_0 q_k$ where, y0 is the initial Yukawa coupling. q is the suppression factor per gear. k is the gear index. In the plot, we have used:

- $y_0 = 1$
- q = 2
- k ranges from 0 to 10

For instance:

- At k = 0, $y_{eff} = 1$
- At k = 5, $y_{eff} = 1/2^5 = 1/32 \approx 0.03125$
- At k = 10, yeff = $1/2^{10} = 1/1024 \approx 0.0009766$

3.3. Dark Matter

Clockwork fermions [10] can also play a role in dark matter models [11–13], providing a mechanism for generating the correct relic abundance and explaining the properties of dark matter particles. In clockwork dark matter models, the dark matter candidate is part of a clockwork chain, with its interactions suppressed by the clockwork mechanism. Consider a clockwork chain for dark matter fermions χi , with the Lagrangian:

$$\mathcal{L} = \sum_{i=0}^{N} \overline{\chi}_i i\gamma^\mu \partial_\mu \chi_i - \sum_{i=0}^{N-1} m(\overline{\chi}_i \chi_{i+1} + \text{h.c.}), \tag{14}$$

where m is the mass parameter.

The effective mass meff and coupling geff of the lightest fermion ψ0 can be expressed as:

$$m_{\text{eff}} \sim q^{-N} m$$

$$g_{\text{eff}} \sim q^{-N} g$$

The scattering cross-section σ for direct detection experiments is given by:

$$\sigma \propto \frac{g_{\text{eff}}^2}{m_{\text{eff}}^2}$$

The annihilation cross-section ⟨σv⟩ relevant for indirect detection is:

$$\langle \sigma v \rangle \propto \frac{g_{\text{eff}}^4}{m_{\text{eff}}^2}$$

Both cross-sections depend on the effective coupling and mass of the dark matter particle, which are exponentially suppressed in the clockwork model.

3.4. Clockwork Axions

The clockwork mechanism can naturally generate a large effective axion decay constant fa from a series of interacting fields with smaller decay constants. Consider a series of axion fields ai (i = 0, 1, . . . , N) with the following potential:

$$V = \sum_{i=0}^{N-1} \left(\frac{1}{2} m_i^2 (a_{i+1} - q a_i)^2 \right)$$

where q is the clockwork gear ratio and mi are the masses of the intermediate axion fields. The physical axion aphys is a linear combination of the a_i fields and has an effective decay constant given by fphys = q^N f , where f is the decay constant of the original axion field

In Figure 4 the horizontal axis represents the distance from the dark matter source and the vertical axis represents the production rate of the byproducts. The production rates of the byproducts are modeled with power-law functions to represent the decreasing influence over distance:

- **Gamma Rays**: Modeled by the function $\gamma(x) = \rho_{\text{DM}} \cdot \sigma_{\text{ann}} \cdot \left(\frac{1}{1+x}\right)^2$
- **Neutrinos**: Modeled by the function $\nu(x) = \rho_{\text{DM}} \cdot \Gamma_{\text{decay}} \cdot \left(\frac{1}{1+x}\right)^{1.5}$
- **Positrons**: Modeled by the function $e^+(x) = \rho_{\text{DM}} \cdot \sigma_{\text{ann}} \cdot \left(\frac{1}{1+x}\right)^{1.2}$

Where:

- ρ_{DM} is the dark matter density.
- σ_{ann} is the annihilation cross-section.
- Γ_{decay} is the decay rate.

Figure 4 shows the production rates of gamma rays, neutrinos, and positrons as a function of distance from the dark matter source:

- **Gamma Rays** (Blue): The production rate decreases with a power-law suppression of $(1/(1+x))^2$.
- **Neutrinos** (Red): The production rate decreases with a power-law suppression of $(1/(1+x))^{1.5}$.
- **Positrons** (Green): The production rate decreases with a power-law suppression of $(1/(1+x))^{1.2}$.

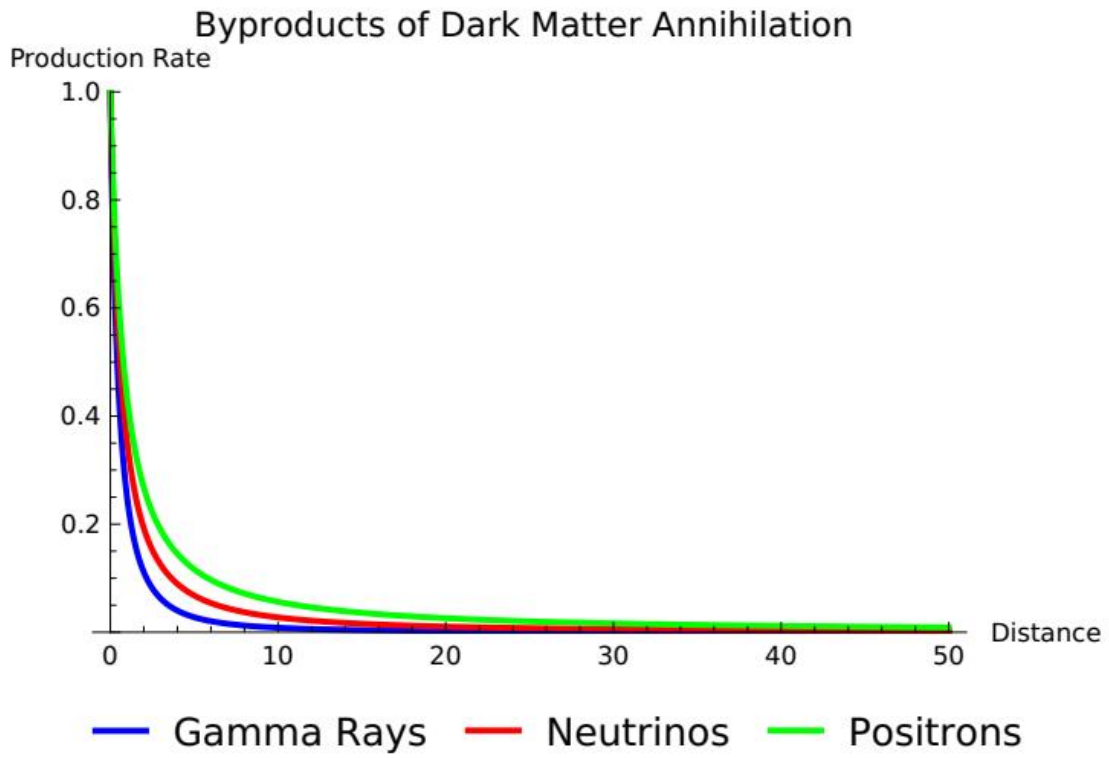

Figure 4. Figure 4 illustrates the production rates of various byproducts (gamma rays, neutrinos, and positrons) resulting from dark matter annihilation in astrophysical environments, modeled using a power-law suppression function rather than an exponential one.

In Figure 5, the horizontal axis represents the distance from the dark matter source and the vertical axis represents the energy of the gamma rays. The production rate of gamma rays is modeled with a power-law function to represent the decreasing influence over distance and energy:

$$\gamma(x, y) = \rho_{\text{DM}} \cdot \sigma_{\text{ann}} \cdot \left(\frac{1}{1 + x + y} \right)^2$$

where:

- ρ_{DM} is the dark matter density.
- σ_{ann} is the annihilation cross-section.
- x is the distance from the dark matter source.
- y is the energy of the gamma rays.

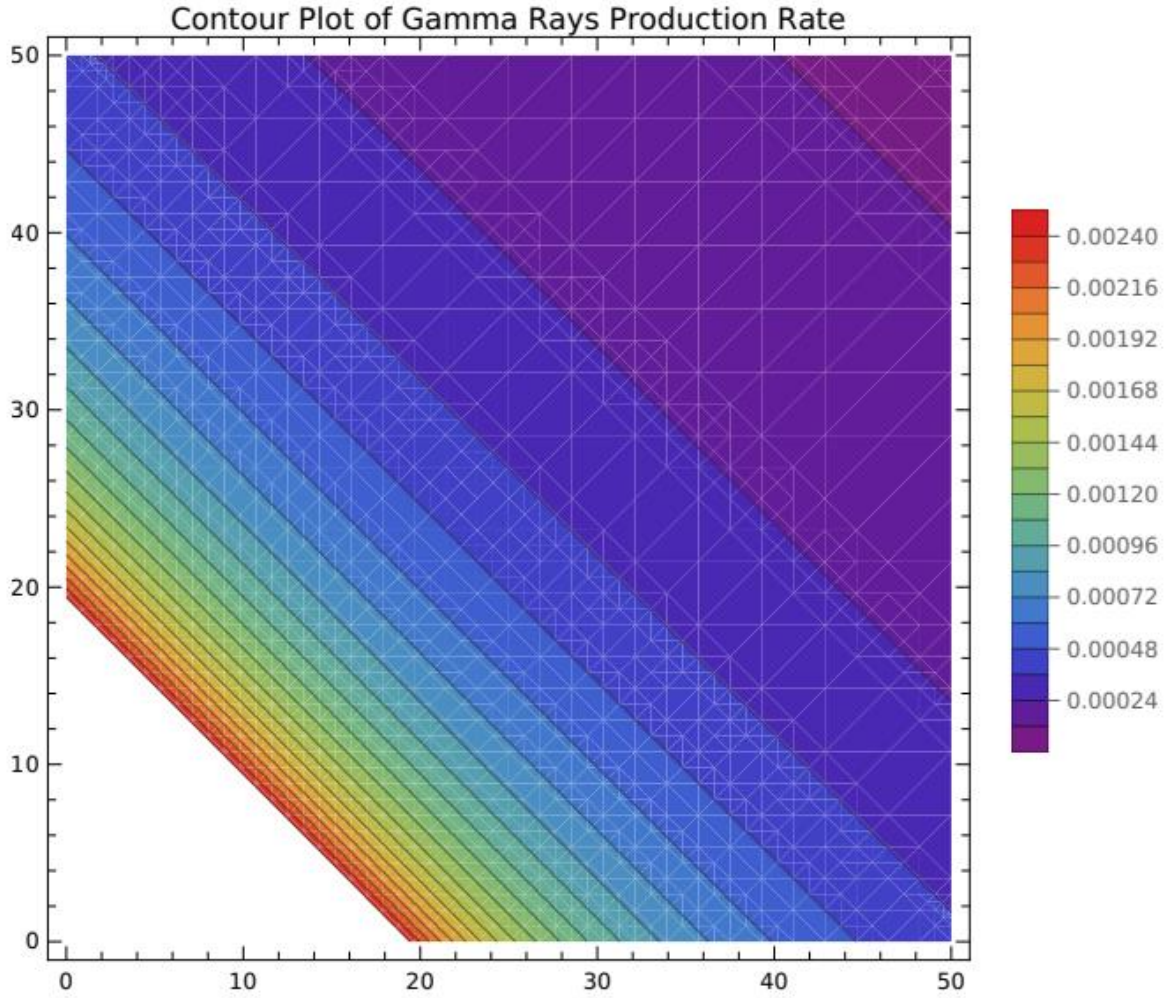

Figure 5. Figure 5 illustrates the production rate of gamma rays resulting from dark matter annihilation in astrophysical environments, modeled using a power-law suppression function.

In Figure 6 the horizontal axis represents the distance from the dark matter source. The horizontal axis represents the energy of the gamma rays. The vertical axis represents the production rate of the gamma rays. The production rate of gamma rays is modeled with a power-law function to represent the decreasing influence over distance and energy:

$$\gamma(x,y) = \rho_{\mathrm{DM}} \cdot \sigma_{\mathrm{ann}} \cdot \left(\frac{1}{1+x+y}\right)^2$$

where:

- ρ_{DM} is the dark matter density.
- σ_{ann} is the annihilation cross-section.
- x is the distance from the dark matter source.
- y is the energy of the gamma rays.

The 3D plot shows the production rate of gamma rays as a function of distance and energy. The surface color represents different levels of production rates, with a rainbow color scheme indicating higher production rates in warmer colors (e.g., red) and lower production rates in cooler colors (e.g., blue)

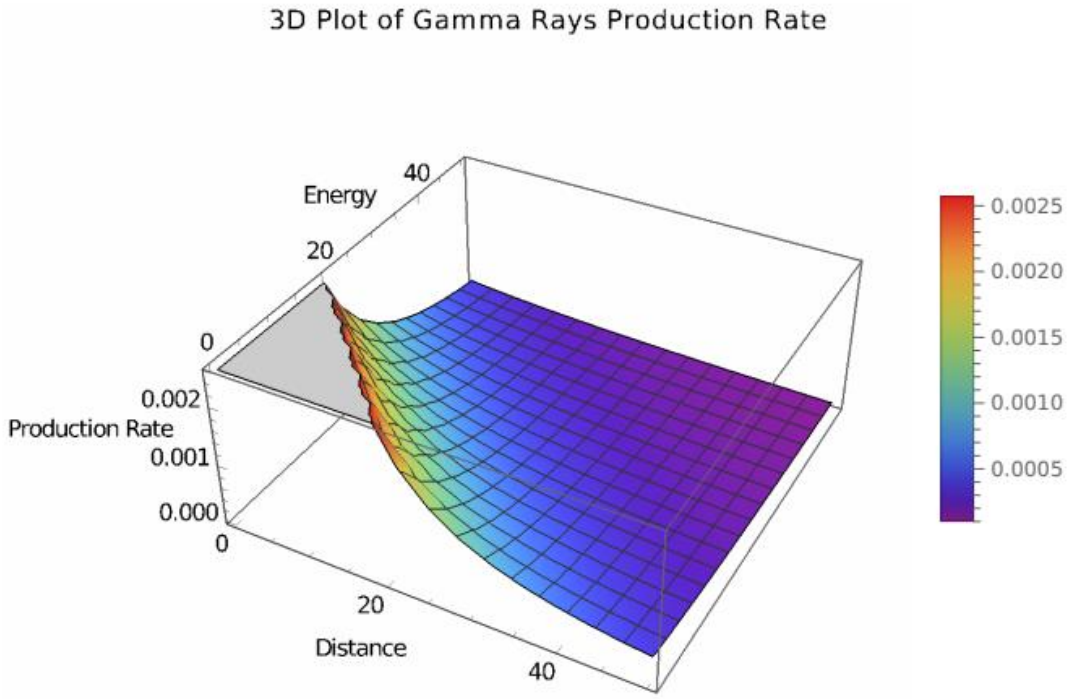

Figure 6. In Figure 6 the 3D plot illustrates the production rate of gamma rays resulting from dark matter annihilation in astrophysical environments, modeled using a power-law suppression function.

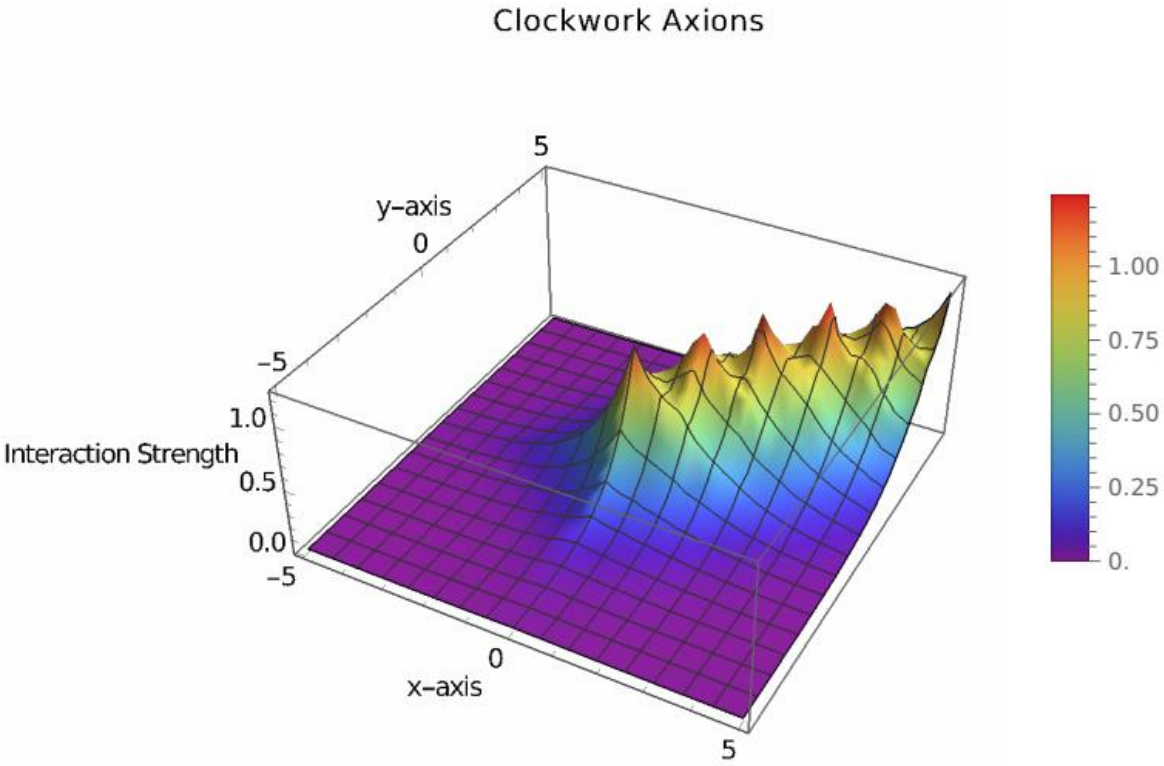

Figure 7. Figure 7 illustrates the conceptual model of clockwork axions using the clockwork fermion model. The plot shows how the interaction strength varies in a 3D space.

Figure 7 is generated using a function that describes the interaction of clockwork axions in a 3D space:

$$f(x,y) = \sum_{k=0}^{n} \exp(-c|x-k|) \cdot \exp(-c|y-k|)$$

where:

- c is the clockwork factor, which controls the exponential decay.
- n is the number of sites in the clockwork chain.
- x and y are variables representing the spatial dimensions.

3.4.4. Implementation of Clockwork in Higher Dimensions

In higher-dimensional theories [14–16] , the clockwork mechanism can be implemented by considering fields that propagate in the extra dimensions.

For simplicity, consider a five-dimensional theory with one extra spatial dimension compactified on a circle of radius R.

3.4.5. Clockwork Scalar Fields

The clockwork mechanism can be applied to scalar fields propagating in the extra dimension. Let Φ(x, y) be a scalar field, where x represents the four-dimensional spacetime coordinates and y is the coordinate of the extra dimension. The Lagrangian can be written as:

$$\mathcal{L} = \int_0^{2\pi R} dy \left[\frac{1}{2}\partial_M \Phi \partial^M \Phi - \frac{1}{2} m^2 \Phi^2 - \frac{1}{2} \sum_{n=1}^{N} m_n^2 (\Phi_n - q\Phi_{n-1})^2 \right]$$

3.4.6. Clockwork Gauge Fields

Clockwork mechanisms can also be applied to gauge fields in higher-dimensional theories. Consider a gauge field AM(x, y) in five dimensions. The clockwork Lagrangian for the gauge field can be expressed as:

$$\mathcal{L} = \int_0^{2\pi R} dy \left[-\frac{1}{4} F_{MN} F^{MN} - \frac{1}{2} \sum_{n=1}^{N} m_n^2 (A_n - q A_{n-1})^2 \right]$$

4. Fermion Clockwork

For fermions, the clockwork mechanism can be implemented by considering a chain of Dirac fermions ψi (i = 0, 1, . . . , N) with interactions:

$$\mathcal{L} = \sum_{i=0}^{N} \bar{\psi}_i (i \not{\partial} - m)\psi_i - \sum_{i=0}^{N-1} \left(\frac{m}{2} \bar{\psi}_{i+1} \psi_i + \text{h.c.} \right)$$

Here, ψ_i represents the Dirac fermions, and m is the mass parameter. The physical fermion ψ_{phys} is a linear combination of the fermion fields, resulting in an effective mass or coupling that can be exponentially controlled.

In Figure 8, x-axis represents one component of the field strength. y-axis represents another component of the field strength and z-axis represents the strength of the interaction. Figure 8 is generated using a function that describes the interaction of the Clockwork theory in a 3D space:

$$f(x,y) = \sum_{k=0}^{n} \sin^2(c(x-k)) \cdot \cos^2(c(y-k))$$

physics and cosmology

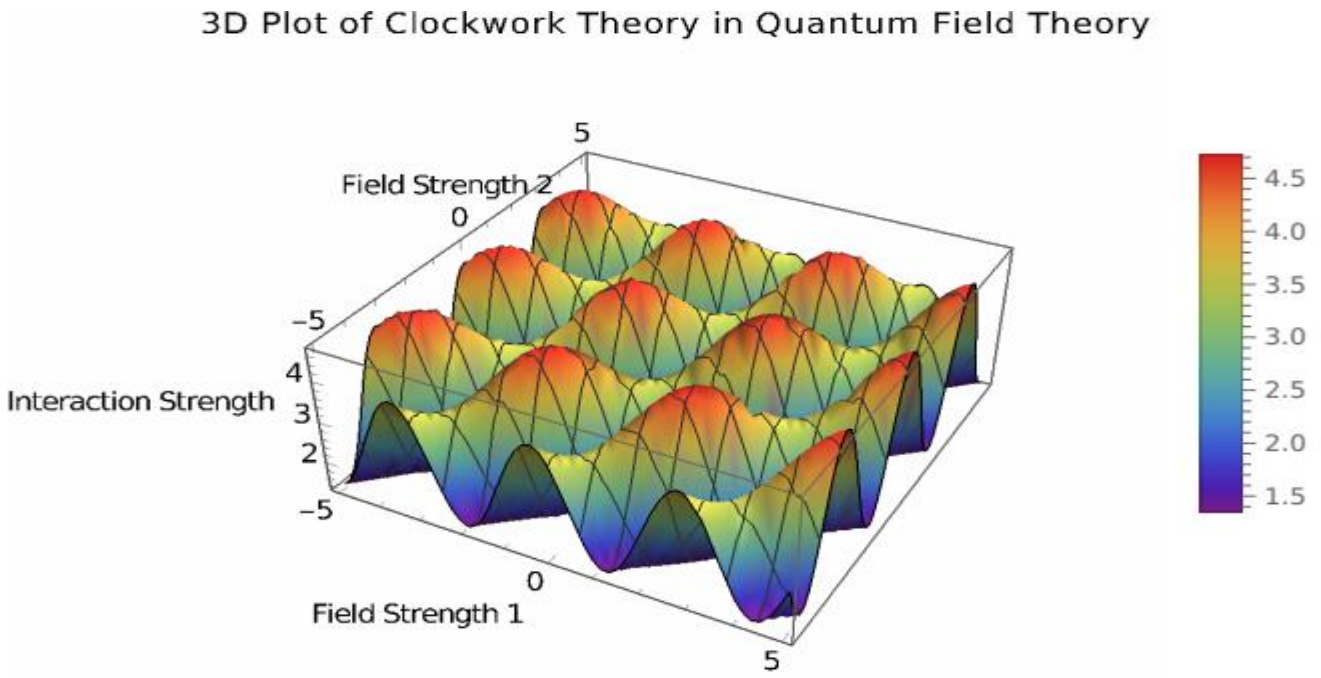

Figure 8. Figure 8 illustrates the conceptual model of the Clockwork theory in quantum field theory (QFT). The plot shows how the interaction strength varies in a 3D space using a sinusoidal and polynomial-based function.

The production cross-section σ for clockwork fermions can be estimated using the parton distribution functions (PDFs) and the matrix elements for the relevant processes. For a Drell-Yan-like process, the cross-section is given by:

$$\sigma(pp \to \psi_i\psi_j) = \int dx_1 dx_2 f_q(x_1, Q^2) f_{\bar{q}}(x_2, Q^2) \hat{\sigma}(q\bar{q} \to \psi_i\psi_j)$$

where f_q and f_q are the PDFs, Q^2 is the momentum transfer squared, and $\hat{\sigma}$ is the partonic cross-section. The decay rate Γ of a heavier clockwork fermion ψ_i into a lighter one ψ_j and a Standard Model particle can be written as:

$$\Gamma(\psi_i \to \psi_j + X) = \frac{|\mathcal{M}|^2}{8\pi m_i}\left(1 - \frac{m_j^2}{m_i^2}\right)^2$$

where |M| is the matrix element for the decay, and mi and mj are the masses of ψi and ψj , respectively. Collider searches for new physics have placed significant constraints on the parameter space of clockwork fermion models.

3. Cosmological Observations: The relic density of the lightest clockwork fermion, if it constitutes dark matter, must be consistent with observations from cosmic microwave background measurements and large-scale structure surveys.

5.2. Cosmological Implications

5.2.1. Dark Matter Candidate

Clockwork fermions, due to their weak interactions and stability, are natural candidates for dark matter. The lightest fermion, ψ_0, has a mass and coupling suppressed by factors of q^{-N}, where q is a parameter greater than 1 and N is the number of fermionic fields. This suppression makes ψ_0 a weakly interacting massive particle (WIMP), which is a leading candidate for dark matter.

5.2.2. Relic Density

. The Boltzmann equation governs this process:

$$\frac{dn_\psi}{dt} + 3Hn_\psi = -\langle \sigma v \rangle (n_\psi^2 - n_{\psi,\text{eq}}^2)$$

where n_ψ is the number density of the dark matter particle, H is the Hubble parameter, $\langle \sigma v \rangle$ is the thermally averaged annihilation cross-section, and n_ψ,eq is the equilibrium number density. The relic density is given by:

$$\Omega_\psi h^2 \approx \frac{1.07 \times 10^9 \text{GeV}^{-1}}{M_{\text{Pl}}} \frac{x_f}{\sqrt{g_*}\langle \sigma v \rangle}$$

where $x_f = m_\psi / T_f$ is the freeze-out temperature, g_* is the number of relativistic degrees of freedom at freeze-out, and MPl is the Planck mass.

5.2.4. Impact on the Cosmic Microwave Background The presence of clockwork fermions affects the Cosmic Microwave Background (CMB) through gravitational interactions and potential annihilation or decay processes.

5.2.5. Experimental Status

Clockwork fermions are being probed through various experimental efforts, including direct detection, indirect detection, and collider searches

5.2.6. Direct Detection Direct detection experiments aim to measure the recoil of nuclei due to collisions with dark matter particles. Notable experiments include:

5.2.7. LUX-ZEPLIN (LZ)

LUX-ZEPLIN is a second-generation dark matter direct detection experiment using a dual-phase xenon detector.

5.2.8. XENONnT

The XENONnT experiment is an upgrade of the XENON1T detector, increasing the target mass and improving background suppression.

5.2.9. Indirect Detection

Indirect detection experiments search for the products of dark matter annihilation or decay, such as gamma rays, neutrinos, or positrons.

5.2.10. Fermi Large Area

Telescope (Fermi-LAT) Fermi-LAT is a space-based gamma-ray telescope that searches for gamma rays from dark matter annihilation in regions with high dark matter density, such as the Galactic center.

5.2.11. IceCube

IceCube is a neutrino observatory located at the South Pole.

5.2.12. Collider Searches

Collider experiments, such as those at the Large Hadron Collider (LHC), search for direct production of clockwork fermions.

5.2.13. ATLAS and CMS

The ATLAS and CMS detectors at the LHC have conducted extensive searches for signs of new particles that could be clockwork fermions..

5.2.14. Current Constraints

The non-observation of clockwork fermions in direct, indirect, and collider searches has placed stringent constraints on the parameter space of the model.

6.0.1. Enhanced Clockwork

Mechanisms New models have been proposed to enhance the original clockwork mechanism. These models include variations with different symmetry structures and interactions, providing a broader framework for understanding mass hierarchies and couplings [23–26].

$$\mathcal{L} = \sum_{i=0}^{N} [\overline{\psi}_i (i\gamma^\mu \partial_\mu - m_i)\psi_i - k\overline{\psi}_i \psi_{i+1}]$$

where ψ_i represents the fermionic fields, m_i are the mass terms, and k is the coupling constant.

6.0.3. Experimental Developments

Experimental efforts have made significant strides in probing the existence of clockwork fermions

6.0.4. Collider Searches

Table 1. Summary of collider constraints on clockwork fermions.

Experiment	Mass Range (GeV)	Constraints
ATLAS	100 - 1000	Exclusion up to 900 GeV
CMS	100 - 1000	Exclusion up to 850 GeV

[1] constraints.

6.0.5. Direct and Indirect Detection

Direct detection experiments, such as XENONnT and LUX-ZEPLIN, have improved sensitivity to WIMP interactions, setting stringent limits on the properties of clockwork dark matter.

6.0.6. Future Directions

The future of clockwork fermion research lies in both theoretical exploration and experimental discovery.

6.0.7. Theoretical Exploration

Future work will likely explore extended models of clockwork mechanisms, including those with additional symmetry structures and higher-dimensional setups.

6.0.8. Connections to Other

Theories Connecting clockwork fermions [29–32] with other theoretical frameworks, such as supersymmetry and string theory.

6.1. Experimental Discovery

6.1.1. Next-Generation Colliders

Next-generation colliders, such as the Future Circular Collider (FCC) and the International Linear Collider (ILC), will offer higher energy and luminosity, increasing the potential for discovering clockwork fermions.

6.1.2. Advanced Detection Techniques

Advancements in detection techniques, including increased detector sensitivity and novel data analysis methods.

6.2. Cosmological Observations

Future cosmological observations, such as those from the James Webb Space Telescope (JWST) and next-generation CMB experiments, will provide more precise data on the early universe and structure formation.

7. Conclusion

This review has summarized the theoretical foundations of the clockwork mechanism, its applications to various fields, and the phenomenological implications of clockwork fermions.

7.1. Theoretical Summary

$$\mathcal{L} = \sum_{i=0}^{N} [\overline{\psi}_i (i\gamma^\mu \partial_\mu - m_i)\psi_i - k\overline{\psi}_i \psi_{i+1}]$$

where ψ_i represents the fermionic fields, m_i are the mass terms, and k is the coupling constant. This setup leads to a spectrum of masses and couplings that can be tuned to address various phenomenological requirements

7.2. Experimental Constraints

Table 2 summarizes the current experimental constraints from major experiments.

Table 2. Summary of experimental constraints on clockwork fermions.

Experiment	Mass Range (GeV)	Constraints
ATLAS	100 - 1000	Exclusion up to 900 GeV
CMS	100 - 1000	Exclusion up to 850 GeV
XENONnT	10 - 1000	WIMP-nucleon cross-section limits
Fermi-LAT	-	Limits on gamma-ray signals from annihilation
IceCube	-	Limits on high-energy neutrinos from annihilation

[1] constraints.

7.3.1. Extended Models and Theoretical Exploration

Exploring extended models of the clockwork mechanism, including those with additional symmetries and higher-dimensional frameworks, will provide deeper insights into the nature of mass hierarchies and couplings.

7.3.2. Next-Generation Colliders

Next-generation colliders, such as the Future Circular Collider (FCC) and the International Linear Collider (ILC), will provide higher energy and luminosity, enhancing the potential for discovering clockwork fermions. These colliders will enable more precise measurements and a broader exploration of the parameter space.

8. Additional Theoretical Details

8.1. Clockwork Mechanism in Higher Dimensions

$$\mathcal{L} = \sum_{i=0}^{N} [\overline{\psi}_i (i\gamma^\mu \partial_\mu - m_i)\psi_i - k\overline{\psi}_i \psi_{i+1}] - \frac{1}{2}\sum_{i=0}^{N} \phi_i^2$$

where φ_i represents the additional scalar fields introduced in the higher-dimensional setup. This modification allows for more complex interactions and mass generation mechanisms.

8.2. Clockwork Mechanism with Non-Abelian Symmetries

Incorporating non-Abelian symmetries into the clockwork mechanism can lead to different types of mass hierarchies.

$$\mathcal{L} = \sum_{i=0}^{N} [\overline{\psi}_i (i\gamma^\mu \partial_\mu - m_i)\psi_i - k\overline{\psi}_i \mathbf{T} \psi_{i+1}]$$

where T represents the generators of the SU(2) symmetry. This results in a more complex mass spectrum and interaction structure.

Table 3. Extended parameter space and current experimental bounds on clockwork fermions.

Experiment	Parameter	Range	Current Bounds
LUX-ZEPLIN	σ_{nucleon}	$10^{-47} - 10^{-45}$ cm^2	Constraints up to 10^{-46} cm^2
XENONnT	σ_{nucleon}	$10^{-47} - 10^{-45}$ cm^2	Constraints up to 10^{-46} cm^2
Fermi-LAT	σv	$10^{-25} - 10^{-23}$ cm^3/s	Limits on σv
IceCube	σv	$10^{-25} - 10^{-23}$ cm^3/s	Limits on σv

[1] extended constraints.

9. Discussion

The Clockwork Fermion model has significantly advanced our understanding of the hierarchical structure of fermion masses and mixings.

9.1. Implications of Findings

The findings from our review underscore the versatility and robustness of the Clockwork Fermion model. Its ability to provide a natural explanation for the smallness of neutrino masses without invoking unnaturally small Yukawa couplings has significant implications for neutrino physics and beyond. Moreover, the model's predictions about the existence of new particles at scales accessible to current or near-future experiments open exciting possibilities for discovery at the Large Hadron Collider (LHC) and other experimental facilities.

In the broadest context, the Clockwork Fermion model not only addresses specific issues related to fermion masses but also offers insights into the unification of forces and the structure of space-time at fundamental levels. **9.2. Future**

Research Directions

While the Clockwork Fermion model has achieved considerable success in explaining certain phenomena, several areas warrant further investigation:

- Detailed Phenomenological Studies

- Cosmological Implications:

• Axion field nonhomogeneities can lead to primordial nonlinear structures facilitating galaxy formation at $z > 10$ [35].

• Extensions and Modifications: The development of extended or modified versions of the Clockwork model, including those that integrate other theoretical frameworks such as string theory or holography, could provide a deeper understanding of its foundational principles.

• Experimental Tests: Designing and implementing experimental setups that can specifically test the predictions of the Clockwork Fermion model is crucial.

References

1. Giudice, G. F.; McCullough, M. A Clockwork Theory, J. High Energy Phys. 2017, 02, 036. doi.org/10.1007/JHEP02(2017)036
2. 2. Batell, B.; Giudice G.F; McCullough, M. Natural heavy supersymmetry, JHEP 2015, 12, 162 [arXiv:1509.00834] [INSPIRE].
3. 3. Choi, K.; Im, S.H. Realizing the relaxion from multiple axions and its UV completion with high scale supersymmetry, JHEP, 2016, 01, 149 [arXiv:1511.00132] [INSPIRE].
4. 4. Patel, K.M. Clockwork mechanism for flavor hierarchies, Phys. Rev. D, 2017, 96, 115013 [arXiv:1711.05393] [INSPIRE].
5. 5. Craig, N.; Sutherland, D. Exponential hierarchies from Anderson localization in theory space, Phys. Rev. Lett., 2018, 120, 221802 [arXiv:1710.01354] [INSPIRE]
6. 6. Kaplan, D.E.; Rattazzi, R. Large field excursions and approximate discrete symmetries from a clockwork axion, Phys. Rev. D, 2016, 93, 085007 [arXiv:1511.01827] [INSPIRE].
7. 7. Keren-Zur, B.; Lodone, P.; Nardecchia, M.; Pappadopulo, D.; Rattazzi, R.; Vecchi, L. On partial compositeness and the CP asymmetry in charm decays, Nucl. Phys. B, 2013, 867, 394 [arXiv:1205.5803] [INSPIRE].
8. 8. Randall, L.; Sundrum, R. A large mass hierarchy from a small extra dimension, Phys. Rev. Lett., 1999, 83, 3370 [hep-ph/9905221] [INSPIRE].
9. 9. Lee, H.M. Gauged U(1) clockwork theory, Phys. Lett. B, 2018, 778, 79, [arXiv:1708.03564] [INSPIRE].
10. 10. Ghosh, G. Majorana Neutrinos and Clockworked Yukawa Couplings Contribution to Nonobservation of the Rare Leptonic Decay $l\,i \rightarrow l\,j + \gamma$, Clockwork, LHEP 2023, 2023, 351, doi:10.31526/LHEP.2023.351;
11. 11. Kim, J.; McDonald, J. Clockwork Higgs portal model for freeze-in dark matter, Phys. Rev. D , 2018, 98, 023533 [arXiv:1709.04105] [INSPIRE].
12. 12. Folgado, M.G.; Donini, A.; Rius, N. Gravity-mediated dark matter in clockwork/linear dilaton extradimensions, JHEP, 2020, 04, 036, [arXiv:1912.02689] [INSPIRE].
13. 13. Kang, Y.-J.; Lee, H.M. Lightening gravity-mediated dark matter, Eur. Phys. J. C, 2020, 80, 602, [arXiv:2001.04868] [INSPIRE].
14. 14. Folgado, M.G.; Donini, A.; Rius, N. Gravity-mediated dark matter in clockwork/linear dilaton extradimensions, JHEP, 2020, 036 [arXiv:1912.02689] [INSPIRE].
15. 15. Antoniadis, I.; Arkani-Hamed, N.; Dimopoulos, S., Dvali, G.R. New dimensions at a millimeter to a Fermi and superstrings at a TeV, Phys. Lett. B, 1998, 436, 257 [hep-ph/9804398] [INSPIRE].

16. Arkani-Hamed, N.; Dimopoulos, S.; Dvali, G.R. The hierarchy problem and new dimensions at a millimeter, Phys. Lett. B, 1998 429, 263, [hep-ph/9803315] [INSPIRE].
17. Gherghetta, T.; Pomarol, A. Bulk fields and supersymmetry in a slice of AdS, Nucl. Phys. B 2000, 586, 141 [hep-ph/0003129] [INSPIRE].
18. Farakos, K.; Kehagias, A.; Koutsoumbas, G.; Gauge field localization in the linear dilaton background, Phys. Lett. B, 2020, 807, 135549 [arXiv:2004.14856] [INSPIRE]. 19. von Gersdorff, G. Realistic GUT Yukawa couplings from a random clockwork model, [arXiv:2005.14207] [INSPIRE].
20. Giudice, G.F.; Kats, Y.; McCullough, M.; Torre, R.; Urbano, A. Clockwork/linear dilaton: structure and phenomenology, JHEP 06, 2018, 009 [arXiv:1711.08437] [INSPIRE].
21. Ben-Dayan, I. Generalized clockwork theory, Phys. Rev. D, 2019, 99, 096006.
22. Lee, H.M.; Park, M.; Sanz, V. Gravity-mediated (or composite) dark matter confronts astrophysical data, JHEP, 2014, 05, 063 [arXiv:1401.5301] [INSPIRE].
23. Arkani-Hamed, N.; Dimopoulos, S.; Dvali, G.R. The hierarchy problem and new dimensions at a millimeter, Phys. Lett. B, 1998, 429, 263 [hep-ph/9803315] [INSPIRE].
24. Kehagias, A.; Riotto, A. The Clockwork Supergravity, JHEP, 2018, 02, 160.
25. Kang, YJ.; Kim, S.; Lee, H.M. The Clockwork Standard Model. J. High Energ. Phys, (2020), 005.
26. Babu, K. S.; Saad, S. Flavor hierarchies from clockwork in SO (10) GUT, Phys. Rev. D, 103, 015009.
27. Wood, K. M.; Saffin, P.; Avgoustidis, A. Clockwork Cosmology, JCAP , 2023, 07, 062.
28. Choi, K.; Hui Im, S.; Sub Shin, C. General Continuum Clockwork, JHEP, 2018 , 07. 113.
29. Kitabayashi, T. Clockwork origin of neutrino mixings, Phys.Rev.D, 2019, 100 , 3, 035019.
30. Farina, M.; Pappadopulo, D.; Rompineve, F., Tesi, A. The photo-philic QCD axion, JHEP, 2017 01, 095.
31. Kehagias, A.; Riotto, A. The Clockwork Supergravity, JHEP, 2018, 02 , 160.
32. Ben-Dayan, I. Generalized Clockwork Theory, Phys.Rev.D, 2019, 99, 9, 096006, arXiv: 1706.05308.
33. Craig, N.; Garcia Garcia, I.; Sutherland, D. Disassembling the Clockwork Mechanism, JHEP, 2017, 10, 018.
34. Kitajima, N.; Takahashi, F., Resonant production of dark photons from axions without a large coupling, Phys.Rev.D 2023, 107, 12, 123518, arXiv: 2303.05492.
35. Khlopov, M. What comes after the Standard Model? Prog. Part. Nucl. Phys. 2020, 116, 103824.

Thank you for your attention